CHAPTER

7 Binary Systems and Stellar Parameters

7.1 ■ THE CLASSIFICATION OF BINARY STARS

A detailed understanding of the structure and evolution of stars (the goal of Part II) requires knowledge of their physical characteristics. We have seen that knowledge of blackbody radiation curves, spectra, and parallax enables us to determine a star's effective temperature, luminosity, radius, composition, and other parameters. However, the only direct way to determine the mass of a star is by studying its gravitational interaction with other objects.

In Chapter 2 Kepler's laws were used to calculate the masses of members of our Solar System. However, the universality of the gravitational force allows Kepler's laws to be generalized to include the orbits of stars about one another and even the orbital interactions of galaxies, as long as proper care is taken to refer all orbits to the center of mass of the system.

Fortunately, nature has provided ample opportunity for astronomers to observe binary star systems. At least half of all "stars" in the sky are actually multiple systems, two or more stars in orbit about a common center of mass. Analysis of the orbital parameters of these systems provides vital information about a variety of stellar characteristics, including mass.

The methods used to analyze the orbital data vary somewhat depending on the geometry of the system, its distance from the observer, and the relative masses and luminosities of the components. Consequently, binary star systems are classified according to their specific observational characteristics.

- **Optical double**. These systems are not actually binaries at all but simply two stars that lie along the same line of sight (i.e., they have similar right ascensions and declinations). As a consequence of their large physical separations, the stars are not gravitationally bound, and hence the system is not useful in determining stellar masses.

- **Visual binary**. Both stars in the binary can be resolved independently, and if the orbital period is not prohibitively long, it is possible to monitor the motion of each member of the system. These systems provide important information about the angular separation of the stars from their mutual center of mass. If the distance to the binary is also known, the linear separations of the stars can then be calculated.

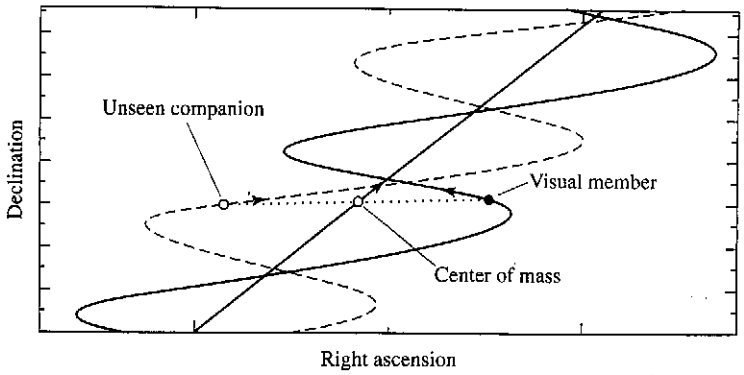

FIGURE 7.1 An astrometric binary, which contains one visible member. The unseen component is implied by the oscillatory motion of the observable star in the system. The proper motion of the entire system is reflected in the straight-line motion of the center of mass.

- **Astrometric binary**. If one member of a binary is significantly brighter than the other, it may not be possible to observe both members directly. In such a case the existence of the unseen member may be deduced by observing the oscillatory motion of the visible component. Since Newton's first law requires that a constant velocity be maintained by a mass unless a force is acting upon it, such an oscillatory behavior requires that another mass be present (see Fig. 7.1).

- **Eclipsing binary**. For binaries that have orbital planes oriented approximately along the line of sight of the observer, one star may periodically pass in front of the other, blocking the light of the eclipsed component (see Fig. 7.2). Such a system is recognizable by regular variations in the amount of light received at the telescope. Not only do observations of these *light curves* reveal the presence of two stars, but the data can also provide information about relative effective temperatures and radii of each star based on the depths of the light curve minima and the lengths of the eclipses. Details of such an analysis will be discussed in Section 7.3.

- **Spectrum binary**. A spectrum binary is a system with two superimposed, independent, discernible spectra. The Doppler effect (Eq. 4.35) causes the spectral lines of a star to be shifted from their rest frame wavelengths if that star has a nonzero radial velocity. Since the stars in a binary system are constantly in motion about their mutual center of mass, there must necessarily be periodic shifts in the wavelength of every spectral line of each star (unless the orbital plane is exactly perpendicular to the line of sight, of course). It is also apparent that when the lines of one star are blueshifted, the lines of the other must be redshifted relative to the wavelengths that would be produced if the stars were moving with the constant velocity of the center of mass. However, it may be that the orbital period is so long that the time dependence of the spectral wavelengths is not readily apparent. In any case, if one star is not overwhelmingly more luminous than its companion and if it is not possible to resolve each star separately, it may still be possible to recognize the object as a binary system by observing the superimposed and oppositely Doppler-shifted spectra.

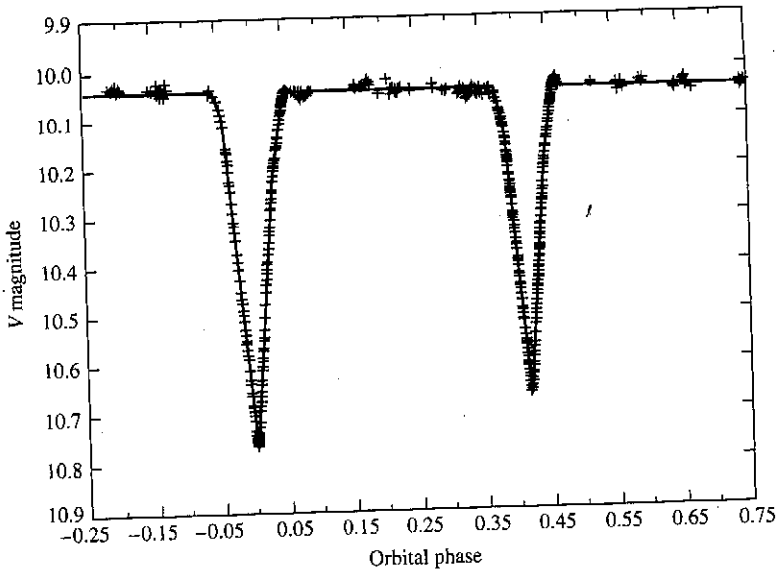

FIGURE 7.2 The V magnitude light curve of YY Sagittarii, an eclipsing binary star. The data from many orbital periods have been plotted on this light curve as a function of phase, where the phase is defined to be 0.0 at the primary minimum. This system has an orbital period $P = 2.6284734$ d, an eccentricity $e = 0.1573$, and orbital inclination $i = 88.89°$ (see Section 7.2). (Figure adopted from Lacy, C. H. S., *Astron. J.*, *105*, 637, 1993.)

Even if the Doppler shifts are not significant (if the orbital plane is perpendicular to the line of sight, for instance), it may still be possible to detect two sets of superimposed spectra if they originate from stars that have significantly different spectral features (see the discussion of spectral classes in Section 8.1).

- **Spectroscopic binary**. If the period of a binary system is not prohibitively long and if the orbital motion has a component along the line of sight, a periodic shift in spectral lines will be observable. Assuming that the luminosities of the stars are comparable, both spectra will be observable. However, if one star is much more luminous than the other, then the spectrum of the less luminous companion will be overwhelmed and only a single set of periodically varying spectral lines will be seen. In either situation, the existence of a binary star system is revealed. Figure 7.3 shows the relationship between spectra and orbital phase for a spectroscopic binary star system.

These specific classifications are not mutually exclusive. For instance, an unresolved system could be both an eclipsing and a spectroscopic binary. It is also true that some systems can be significantly more useful than others in providing information about stellar characteristics. Three types of systems can provide us with mass determinations: visual binaries combined with parallax information; visual binaries for which radial velocities are available over a complete orbit; and eclipsing, double-line, spectroscopic binaries.

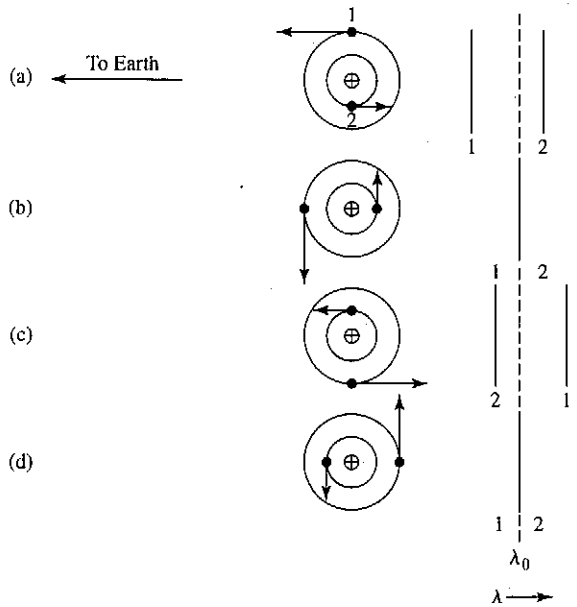

FIGURE 7.3 The periodic shift in spectral features of a double-line spectroscopic binary. The relative wavelengths of the spectra of Stars 1 and 2 are shown at four different phases during the orbit: (a) Star 1 is moving toward the observer while Star 2 is moving away. (b) Both stars have velocities perpendicular to the line of sight. (c) Star 1 is receding from the observer while Star 2 is approaching. (d) Again both stars have velocities perpendicular to the line of sight. λ_0 represents the wavelength of the observed line Doppler-shifted by the velocity of the center of mass of the system.

7.2 ■ MASS DETERMINATION USING VISUAL BINARIES

When the angular separation between components of a binary system is greater than the resolution limit imposed by local seeing conditions and the fundamental diffraction limitation of the Rayleigh criterion, it becomes possible to analyze the orbital characteristics of the individual stars. From the orbital data, the orientation of the orbits and the system's center of mass can be determined, providing knowledge of the ratio of the stars' masses. If the distance to the system is also known, from trigonometric parallax for instance, the linear separation of the stars can be determined, leading to the individual masses of the stars in the system.

To see how a visual binary can yield mass information, consider two stars in orbit about their mutual center of mass. Assuming that the orbital plane is perpendicular to the observer's line of sight, we see from the discussion of Section 2.3 that the ratio of masses may be found from the ratio of the angular separations of the stars from the center of mass. Using Eq. (2.19) and considering only the lengths of the vectors $\mathbf{r}_1$ and $\mathbf{r}_2$, we find that

$$\frac{m_1}{m_2} = \frac{r_2}{r_1} = \frac{a_2}{a_1}, \tag{7.1}$$

where a_1 and a_2 are the semimajor axes of the ellipses. If the distance from the observer to

the binary star system is d, then the angles subtended by the semimajor axes are

$$\alpha_1 = \frac{a_1}{d} \qquad \text{and} \qquad \alpha_2 = \frac{a_2}{d},$$

where α_1 and α_2 are measured in radians. Substituting, we find that the mass ratio simply becomes

$$\boxed{\frac{m_1}{m_2} = \frac{\alpha_2}{\alpha_1}.} \tag{7.2}$$

Even if the distance to the star system is not known, the mass ratio may still be determined. Note that since only the ratio of the subtended angles is needed, α_1 and α_2 may be expressed in arcseconds, the unit typically used for angular measure in astronomy.

The general form of Kepler's third law (Eq. 2.37),

$$P^2 = \frac{4\pi^2}{G\,(m_1 + m_2)} a^3,$$

gives the sum of the masses of the stars, provided that the semimajor axis (a) of the orbit of the reduced mass is known. Since $a = a_1 + a_2$ (the proof of this is left as an exercise), the semimajor axis can be determined directly only if the distance to the system has been determined. Assuming that d is known, $m_1 + m_2$ may be combined with m_1/m_2 to give each mass separately.

This process is complicated somewhat by the proper motion of the center of mass[1] (see Fig. 7.1) and by the fact that most orbits are not conveniently oriented with their planes perpendicular to the line of sight of the observer. Removing the proper motion of the center of mass from the observations is a relatively simple process since the center of mass must move at a constant velocity. Fortunately, estimating the orientation of the orbits is also possible and can be taken into consideration.

Let i be the **angle of inclination** between the plane of an orbit and the plane of the sky, as shown in Fig. 7.4; note that the orbits of both stars are necessarily in the same plane. As a special case, assume that the orbital plane and the plane of the sky (defined as being perpendicular to the line of sight) intersect along a line parallel to the minor axis, forming a **line of nodes**. The observer will not measure the actual angles subtended by the semimajor axes α_1 and α_2 but their projections onto the plane of the sky, $\tilde{\alpha}_1 = \alpha_1 \cos i$ and $\tilde{\alpha}_2 = \alpha_2 \cos i$. This geometrical effect plays no role in calculating the mass ratios since the $\cos i$ term will simply cancel in Eq. (7.2):

$$\frac{m_1}{m_2} = \frac{\alpha_2}{\alpha_1} = \frac{\alpha_2 \cos i}{\alpha_1 \cos i} = \frac{\tilde{\alpha}_2}{\tilde{\alpha}_1}.$$

However, this projection effect can make a significant difference when we are using Kepler's third law. Since $\alpha = a/d$ (α in radians), Kepler's third law may be solved for the sum of

[1]The annual wobble of stellar positions due to trigonometric parallax must also be considered, when significant.

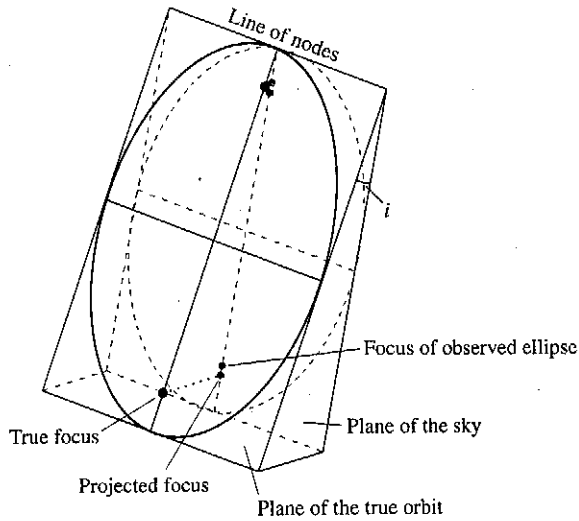

FIGURE 7.4 An elliptical orbit projected onto the plane of the sky produces an observable elliptical orbit. The foci of the original ellipse do not project onto the foci of the observed ellipse, however.

the masses to give

$$m_1 + m_2 = \frac{4\pi^2}{G}\frac{(\alpha d)^3}{P^2} = \frac{4\pi^2}{G}\left(\frac{d}{\cos i}\right)^3 \frac{\tilde{\alpha}^3}{P^2}, \tag{7.3}$$

where $\tilde{\alpha} = \tilde{\alpha}_1 + \tilde{\alpha}_2$.

To evaluate the sum of the masses properly, we must deduce the angle of inclination. This can be accomplished by carefully noting the apparent position of the center of mass of the system. As illustrated in Fig. 7.4, the projection of an ellipse tilted at an angle i with respect to the plane of the sky will result in an observed ellipse with a different eccentricity. However, the center of mass will not be located at one of the foci of the projection—a result that is inconsistent with Kepler's first law. Thus the geometry of the true ellipse may be determined by comparing the observed stellar positions with mathematical projections of various ellipses onto the plane of the sky.

Of course, the problem of projection has been simplified here. Not only can the angle of inclination i be nonzero, but the ellipse may be tilted about its major axis and rotated about the line of sight to produce any possible orientation. However, the general principles already mentioned still apply, making it possible to deduce the true shapes of the stars' elliptical orbits, as well as their masses.

It is also possible to determine the individual masses of members of visual binaries, even if the distance is not known. In this situation, detailed radial velocity data are needed. The projection of velocity vectors onto the line of sight, combined with information about the stars' positions and the orientation of their orbits, provides a means for determining the semimajor axes of the ellipses, as required by Kepler's third law.

7.3 ■ ECLIPSING, SPECTROSCOPIC BINARIES

A wealth of information is available from a binary system even if it is not possible to resolve each of its stars individually. This is particularly true for a double-line, eclipsing, spectroscopic binary star system. In such a system, not only is it possible to determine the individual masses of the stars, but astronomers may be able to deduce other parameters as well, such as the stars' radii and the ratio of their fluxes, and hence the ratio of their effective temperatures. (Of course, eclipsing systems are not restricted to spectroscopic binaries but may occur in other types of binaries as well, such as visual binaries.)

The Effect of Eccentricity on Radial Velocity Measurements

Consider a spectroscopic binary star system for which the spectra of both stars may be seen (a double-line, spectroscopic binary). Since the individual members of the system cannot be resolved, the techniques used to determine the orientation and eccentricity of the orbits of visual binaries are not applicable. Also, the inclination angle i clearly plays a role in the solution obtained for the stars' masses because it directly influences the measured radial velocities. If v_1 is the velocity of the star of mass m_1 and v_2 is the velocity of the star of mass m_2 at some instant, then, referring to Fig. 7.4, the observed radial velocities cannot exceed $v_{1r}^{\max} = v_1 \sin i$ and $v_{2r}^{\max} = v_2 \sin i$, respectively. Therefore, the actual measured radial velocities depend upon the positions of the stars at that instant. As a special case, if the directions of motion of the stars happen to be perpendicular to the line of sight, then the observed radial velocities will be zero.

For a star system having circular orbits, the speed of each star will be constant. If the plane of their orbits lies in the line of sight of the observer ($i = 90°$), then the measured radial velocities will produce sinusoidal *velocity curves*, as in Fig. 7.5. Changing the orbital inclination does not alter the shape of the velocity curves; it merely changes their amplitudes

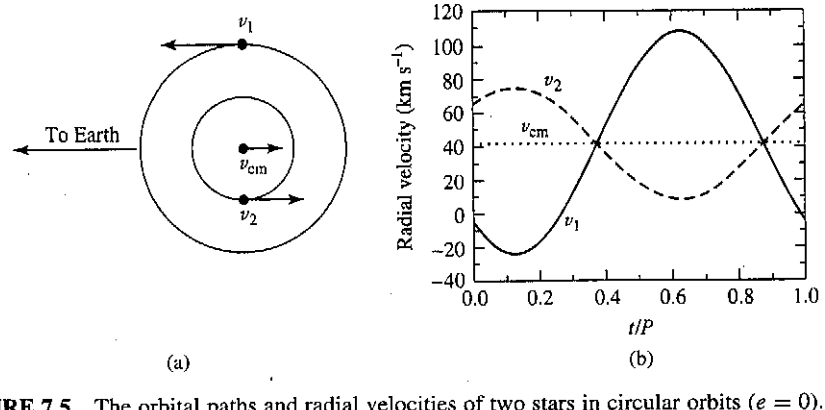

FIGURE 7.5 The orbital paths and radial velocities of two stars in circular orbits ($e = 0$). In this example, $M_1 = 1\ M_\odot$, $M_2 = 2\ M_\odot$, the orbital period is $P = 30$ d, and the radial velocity of the center of mass is $v_{cm} = 42$ km s^{-1}. v_1, v_2, and v_{cm} are the velocities of Star 1, Star 2, and the center of mass, respectively. (a) The plane of the circular orbits lies along the line of sight of the observer. (b) The observed radial velocity curves.

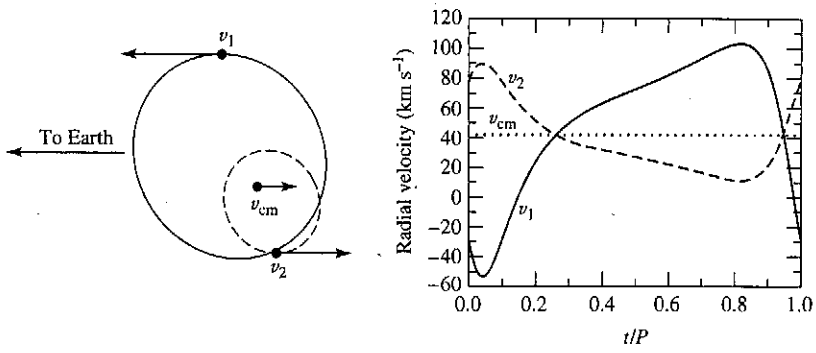

FIGURE 7.6 The orbital paths and radial velocities of two stars in elliptical orbits ($e = 0.4$). As in Fig. 7.5, $M_1 = 1\ M_\odot$, $M_2 = 2\ M_\odot$, the orbital period is $P = 30$ d, and the radial velocity of the center of mass is $v_{cm} = 42$ km s^{-1}. In addition, the orientation of periastron is 45°. v_1, v_2, and v_{cm} are the velocities of Star 1, Star 2, and the center of mass, respectively. (a) The plane of the orbits lies along the line of sight of the observer. (b) The observed radial velocity curves.

by the factor $\sin i$. To estimate i and the actual orbital velocities, therefore, other information about the system is necessary.

When the eccentricity, e, of the orbits is not zero, the observed velocity curves become skewed, as shown in Fig. 7.6. The exact shapes of the curves also depend strongly on the orientation of the orbits with respect to the observer, even for a given inclination angle.

In reality, many spectroscopic binaries possess nearly circular orbits, simplifying the analysis of the system somewhat. This occurs because close binaries tend to circularize their orbits due to tidal interactions over timescales that are short compared to the lifetimes of the stars involved.

The Mass Function and the Mass–Luminosity Relation

If we assume that the orbital eccentricity is very small ($e \ll 1$), then the speeds of the stars are essentially constant and given by $v_1 = 2\pi a_1/P$ and $v_2 = 2\pi a_2/P$ for stars of mass m_1 and m_2, respectively, where a_1 and a_2 are the radii (semimajor axes) and P is the period of the orbits. Solving for a_1 and a_2 and substituting into Eq. (7.1), we find that the ratio of the masses of the two stars becomes

$$\frac{m_1}{m_2} = \frac{v_2}{v_1}. \tag{7.4}$$

Because $v_{1r} = v_1 \sin i$ and $v_{2r} = v_2 \sin i$, Eq. (7.4) can be written in terms of the observed radial velocities rather than actual orbital velocities:

$$\boxed{\frac{m_1}{m_2} = \frac{v_{2r}/\sin i}{v_{1r}/\sin i} = \frac{v_{2r}}{v_{1r}}.} \tag{7.5}$$

As is the situation with visual binaries, we can determine the ratio of the stellar masses without knowing the angle of inclination.

However, as is also the case with visual binaries, finding the sum of the masses does require knowledge of the angle of inclination. Replacing a with

$$a = a_1 + a_2 = \frac{P}{2\pi}(v_1 + v_2)$$

in Kepler's third law (Eq. 2.37) and solving for the sum of the masses, we have

$$m_1 + m_2 = \frac{P}{2\pi G}(v_1 + v_2)^3.$$

Writing the actual radial velocities in terms of the observed values, we can express the sum of the masses as

$$\boxed{m_1 + m_2 = \frac{P}{2\pi G}\frac{(v_{1r} + v_{2r})^3}{\sin^3 i}.} \tag{7.6}$$

It is clear from Eq. (7.6) that the sum of the masses can be obtained only if both v_{1r} and v_{2r} are measurable. Unfortunately, this is not always the case. If one star is much brighter than its companion, the spectrum of the dimmer member will be overwhelmed. Such a system is referred to as a *single-line spectroscopic binary*. If the spectrum of Star 1 is observable but the spectrum of Star 2 is not, Eq. (7.5) allows v_{2r} to be replaced by the ratio of the stellar masses, giving a quantity that is dependent on both of the system masses and the angle of inclination. If we substitute, Eq. (7.6) becomes

$$m_1 + m_2 = \frac{P}{2\pi G}\frac{v_{1r}^3}{\sin^3 i}\left(1 + \frac{m_1}{m_2}\right)^3.$$

Rearranging terms gives

$$\boxed{\frac{m_2^3}{(m_1 + m_2)^2}\sin^3 i = \frac{P}{2\pi G}v_{1r}^3.} \tag{7.7}$$

The right-hand side of this expression, known as the **mass function**, depends only on the readily observable quantities, period and radial velocity. Since the spectrum of only one star is available, Eq. (7.5) cannot provide any information about mass ratios. As a result, the mass function is useful only for statistical studies or if an estimate of the mass of at least one component of the system already exists by some indirect means. If either m_1 or $\sin i$ is unknown, the mass function sets a lower limit for m_2, since the left-hand side is always less than m_2.

Even if both radial velocities are measurable, it is not possible to get exact values for m_1 and m_2 without knowing i. However, since stars can be grouped according to their effective temperatures and luminosities (see Section 8.2), and assuming that there is a relationship between these quantities and mass, then a statistical mass estimate for each class may be found by choosing an appropriately averaged value for $\sin^3 i$. An integral average of $\sin^3 i$ ($\langle \sin^3 i \rangle$) evaluated between 0° and 90° has a value $3\pi/16 \simeq 0.589$.[2] However, since no

[2]The proof is left as an exercise.

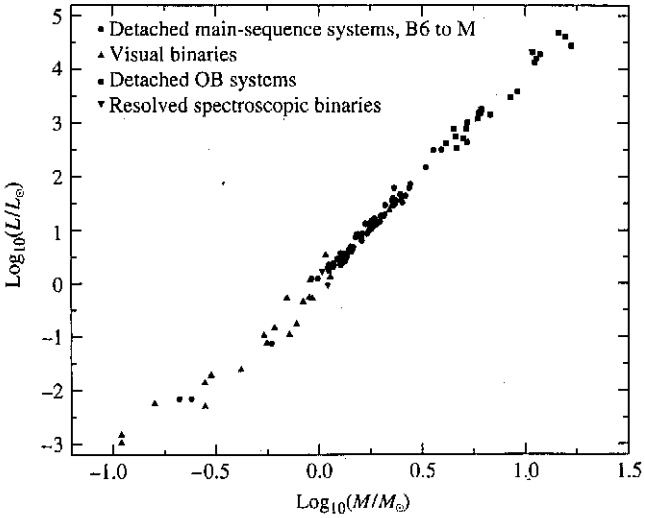

FIGURE 7.7 The mass–luminosity relation. (Data from Popper, *Annu. Rev. Astron. Astrophys.*, *18*, 115, 1980.)

Doppler shift will be noticeable if the inclination angle is very small, it is more likely that a spectroscopic binary star system will be discovered if i differs significantly from 0°. This *selection effect* associated with detecting binary systems suggests that a larger value of $\langle \sin^3 i \rangle \simeq 2/3$ is more representative.

Evaluating masses of binaries has shown the existence of a well-defined **mass–luminosity relation** for the large majority of stars in the sky (see Fig. 7.7). One of the goals of the next several chapters is to investigate the origin of this relation in terms of fundamental physical principles.

Using Eclipses to Determine Radii and Ratios of Temperatures

A good estimate of i is possible in the special situation that a spectroscopic binary star system is observed to be an eclipsing system as well. Unless the distance of separation between the components of the binary is not much larger than the sum of the radii of the stars involved, an eclipsing system implies that i must be close to 90°, as suggested in Fig. 7.8. Even if it were assumed that $i = 90°$ while the actual value was closer to 75°, an error of only 10% would result in the calculation of $\sin^3 i$ and in the determination of $m_1 + m_2$.

From the light curves produced by eclipsing binaries, it is possible to improve the estimate of i still further. Figure 7.9 indicates that if the smaller star is completely eclipsed by the larger one, a nearly constant minimum will occur in the measured brightness of the system during the period of occultation. Similarly, even though the larger star will not be fully hidden from view when the smaller companion passes in front of it, a constant amount of area will still be obscured for a time, and again a nearly constant, though diminished amount of light will be observed. When one star is not completely eclipsed by its companion (Fig. 7.10), the minima are no longer constant, implying that i must be less than 90°.

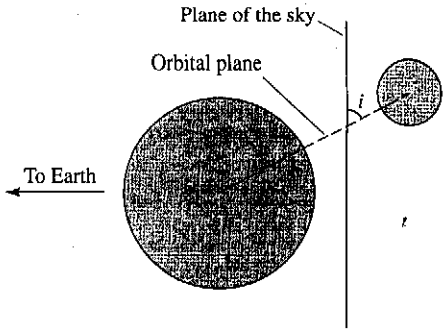

FIGURE 7.8 The geometry of an eclipsing, spectroscopic binary requires that the angle of inclination i be close to 90°.

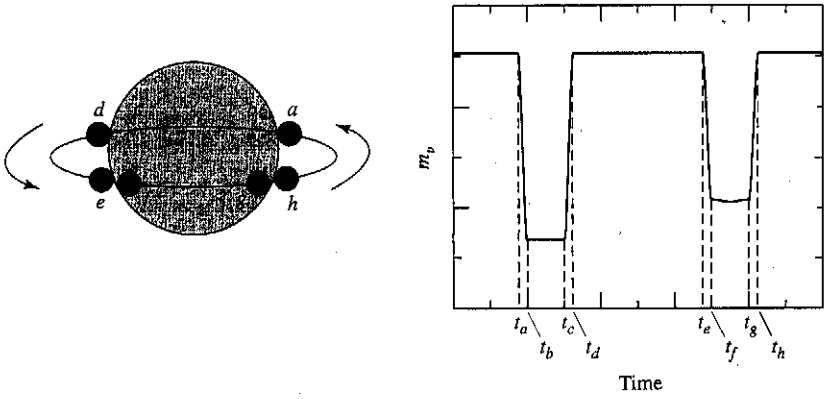

FIGURE 7.9 The light curve of an eclipsing binary for which $i = 90°$. The times indicated on the light curve correspond to the positions of the smaller star relative to its larger companion. It is assumed in this example that the smaller star is hotter than the larger one.

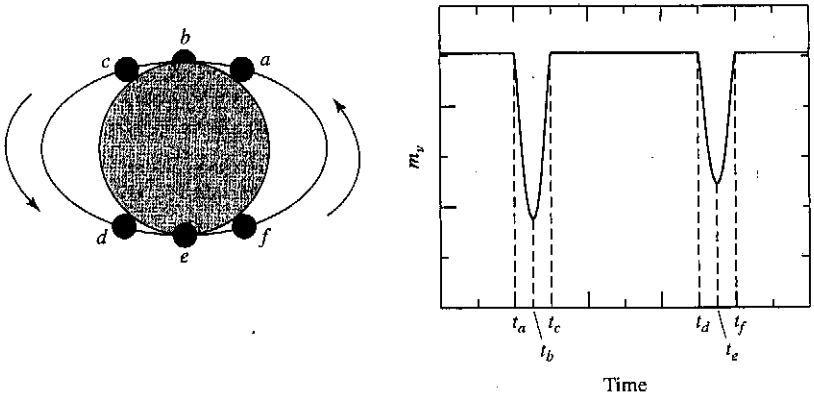

FIGURE 7.10 The light curve of a partially eclipsing binary. It is assumed in this example that the smaller star is hotter than its companion.

Using measurements of the duration of eclipses, it is also possible to find the radii of each member of an eclipsing, spectroscopic binary. Referring again to Fig. 7.9, if we assume that $i \simeq 90°$, the amount of time between *first contact* (t_a) and minimum light (t_b), combined with the velocities of the stars, leads directly to the calculation of the radius of the smaller component. For example, if the semimajor axis of the smaller star's orbit is sufficiently large compared to either star's radius, and if the orbit is nearly circular, we can assume that the smaller object is moving approximately perpendicular to the line of sight of the observer during the duration of the eclipse. In this case the radius of the smaller star is simply

$$r_s = \frac{v}{2}(t_b - t_a), \tag{7.8}$$

where $v = v_s + v_\ell$ is the *relative* velocity of the two stars (v_s and v_ℓ are the velocities of the small and large stars, respectively). Similarly, if we consider the amount of time between t_b and t_c, the size of the larger member can also be determined. It can be quickly shown that the radius of the larger star is just

$$r_\ell = \frac{v}{2}(t_c - t_a) = r_s + \frac{v}{2}(t_c - t_b). \tag{7.9}$$

Example 7.3.1. An analysis of the spectrum of an eclipsing, double-line, spectroscopic binary having a period of $P = 8.6$ yr shows that the maximum Doppler shift of the hydrogen Balmer Hα (656.281 nm) line is $\Delta\lambda_s = 0.072$ nm for the smaller member and only $\Delta\lambda_\ell = 0.0068$ nm for its companion. From the sinusoidal shapes of the velocity curves, it is also apparent that the orbits are nearly circular. Using Eqs. (4.39) and (7.5), we find that the mass ratio of the two stars must be

$$\frac{m_\ell}{m_s} = \frac{v_{rs}}{v_{r\ell}} = \frac{\Delta\lambda_s}{\Delta\lambda_\ell} = 10.6.$$

Assuming that the orbital inclination is $i = 90°$, the Doppler shift of the smaller star implies that the maximum measured radial velocity is

$$v_{rs} = \frac{\Delta\lambda_s}{\lambda} c = 33 \text{ km s}^{-1}$$

and the radius of its orbit must be

$$a_s = \frac{v_{rs} P}{2\pi} = 1.42 \times 10^{12} \text{ m} = 9.5 \text{ AU}.$$

In the same manner, the orbital velocity and radius of the other star are $v_{r\ell} = 3.1$ km s^{-1} and $a_\ell = 0.90$ AU, respectively. Therefore, the semimajor axis of the reduced mass becomes $a = a_s + a_\ell = 10.4$ AU.

continued

The sum of the masses can now be determined from Kepler's third law. If Eq. (2.37) is written in units of solar masses, astronomical units, and years, we have

$$m_s + m_\ell = a^3/P^2 = 15.2\ \mathrm{M}_\odot.$$

Solving for the masses independently yields $m_s = 1.3\ \mathrm{M}_\odot$ and $m_\ell = 13.9\ \mathrm{M}_\odot$.

Furthermore, from the light curve for this system, it is found that $t_b - t_a = 11.7$ hours and $t_c - t_b = 164$ days. Using Eq. (7.8) reveals that the radius of the smaller star is

$$r_s = \frac{(v_{rs} + v_{r\ell})}{2}(t_b - t_a) = 7.6 \times 10^8\ \mathrm{m} = 1.1\ \mathrm{R}_\odot,$$

where one solar radius is $1\ \mathrm{R}_\odot = 6.96 \times 10^8$ m. Equation (7.9) now gives the radius of the larger star, which is found to be $r_\ell = 369\ \mathrm{R}_\odot$.

In this particular system, the masses and radii of the stars are found to differ significantly.

The ratio of the effective temperatures of the two stars can also be obtained from the light curve of an eclipsing binary. This is accomplished by considering the objects as blackbody radiators and comparing the amount of light received during an eclipse with the amount received when both members are fully visible.

Referring once more to the sample binary system depicted in Fig. 7.9, it can be seen that the dip in the light curve is deeper when the smaller, hotter star is passing behind its companion. To understand this effect, recall that the radiative surface flux is given by Eq. (3.18),

$$F_r = F_{\mathrm{surf}} = \sigma T_e^4.$$

Regardless of whether the smaller star passes behind or in front of the larger one, the same total cross-sectional area is eclipsed. Assuming for simplicity that the observed flux is constant across the disks,[3] the amount of light detected from the binary when both stars are fully visible is given by

$$B_0 = k\left(\pi r_\ell^2 F_{r\ell} + \pi r_s^2 F_{rs}\right),$$

where k is a constant that depends on the distance to the system, the amount of intervening material between the system and the detector, and the nature of the detector. The deeper, or *primary*, minimum occurs when the hotter star passes behind the cooler one. If, as in the last example, the smaller star is hotter and therefore has the larger surface flux, and the smaller star is entirely eclipsed, the amount of light detected during the primary minimum may be expressed as

$$B_p = k\pi r_\ell^2 F_{r\ell}$$

while the brightness of the *secondary* minimum is

$$B_s = k\left(\pi r_\ell^2 - \pi r_s^2\right) F_{r\ell} + k\pi r_s^2 F_{rs}.$$

[3] Stars often appear darker near the edges of their disks, a phenomenon referred to as *limb darkening*. This effect will be discussed in Section 9.3.

Since it is generally not possible to determine k exactly, ratios are employed. Consider the ratio of the depth of the primary to the depth of the secondary. Using the expressions for B_0, B_p, and B_s, we find immediately that

$$\frac{B_0 - B_p}{B_0 - B_s} = \frac{F_{rs}}{F_{r\ell}} \tag{7.10}$$

or, from Eq. (3.18),

$$\boxed{\frac{B_0 - B_p}{B_0 - B_s} = \left(\frac{T_s}{T_\ell}\right)^4.} \tag{7.11}$$

Example 7.3.2. Further examination of the light curve of the binary system discussed in Example 7.3.1 provides information on the relative temperatures of the two stars. Photometric observations show that at maximum light the bolometric magnitude is $m_{\text{bol},0} = 6.3$, at the primary minimum $m_{\text{bol},p} = 9.6$, and at the secondary minimum $m_{\text{bol},s} = 6.6$. From Eq. (3.3), the ratio of brightnesses between the primary minimum and maximum light is

$$\frac{B_p}{B_0} = 100^{(m_{\text{bol},0} - m_{\text{bol},p})/5} = 0.048.$$

Similarly, the ratio of brightnesses between the secondary minimum and maximum light is

$$\frac{B_s}{B_0} = 100^{(m_{\text{bol},0} - m_{\text{bol},s})/5} = 0.76.$$

Now, by rewriting Eq. (7.10), we find that the ratio of the radiative fluxes is

$$\frac{F_{rs}}{F_{r\ell}} = \frac{1 - B_p/B_0}{1 - B_s/B_0} = 3.97.$$

Finally, from Eq. (3.18),

$$\frac{T_s}{T_\ell} = \left(\frac{F_{rs}}{F_{r\ell}}\right)^{1/4} = 1.41.$$

A Computer Modeling Approach

The modern approach to analyzing the data from binary star systems involves computing detailed models that can yield important information about a variety of physical parameters. Not only can masses, radii, and effective temperatures be determined, but for many systems other details can be described as well. For instance, gravitational forces, combined with the effects of rotation and orbital motion, alter the stars' shapes; they are no longer simply spherical objects but may become elongated (these effects will be discussed in more detail in Section 18.1). The models may also incorporate information about the nonuniform

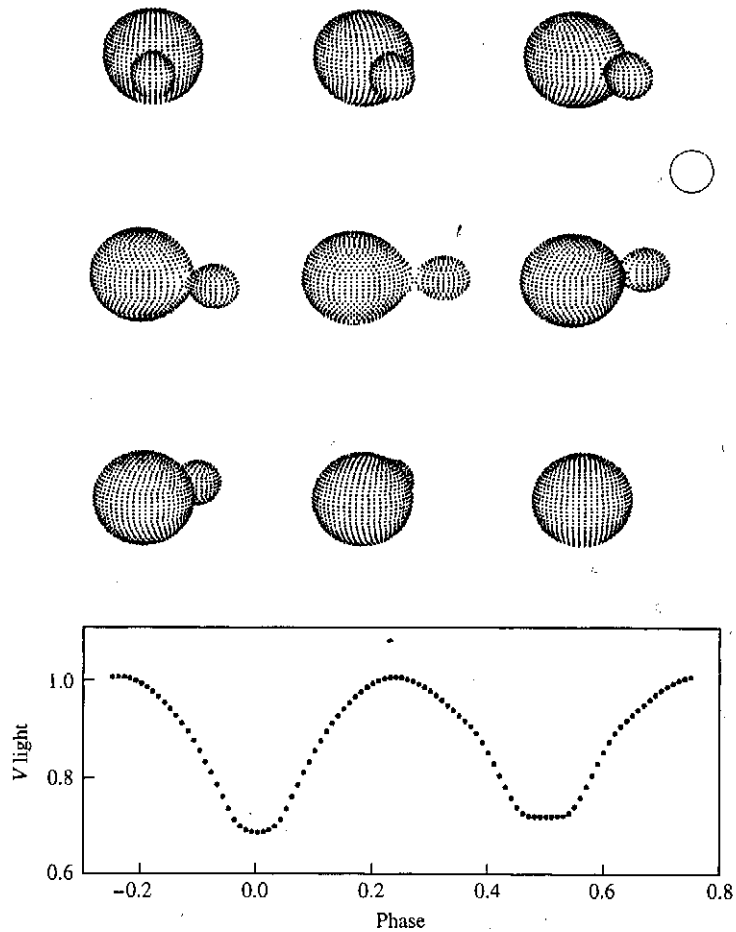

FIGURE 7.11 A synthetic light curve of RR Centauri, an eclipsing binary star system for whicl the two components are in close contact. The open circle represents the size of the Sun. The orbita and physical characteristics of the RR Cen system are $P = 0.6057$ d, $e = 0.0$, $M_1 = 1.8\ M_\odot$, $M_2 = 0.37\ M_\odot$. The spectral classification of the primary is F0V (see Section 8.1 for a discussion of stella spectral classifications). (Figure adapted from R. E. Wilson, *Publ. Astron. Soc. Pac.*, *106*, 921, 1994 ©Astronomical Society of the Pacific.)

distribution of flux across the observed disks of the stars, variations in surface temperatures and so on. Once the shapes of the gravitational equipotential surfaces and other parameters are determined, *synthetic* (theoretical) light curves can be computed for various wavelength bands (U, B, V, etc.), which are then compared to the observational data. Adjustments in the model parameters are made until the light curves agree with the observations. One such model for the binary system RR Centauri is shown in Fig. 7.11. In this system the two stars are actually in contact with each other, producing interesting and subtle effects in the light curve.

In order to introduce you to the process of modeling binary systems, the simple code `TwoStars` is described in Appendix K and available on the companion website. `TwoStars`

makes the simplifying assumption that the stars are perfectly spherically symmetric. Thus `TwoStars` is capable of generating light curves, radial velocity curves, and astrometric data for systems in which the two stars are well separated. The simplifying assumptions imply that `TwoStars` is incapable of modeling the details of more complicated systems such as RR Cen, however.[4]

The study of binary star systems provides valuable information about the observable characteristics of stars. These results are then employed in developing a theory of stellar structure and evolution.

7.4 ■ THE SEARCH FOR EXTRASOLAR PLANETS

For hundreds of years, people have looked up at the night sky and wondered if planets might exist around other stars.[5] However, it wasn't until October 1995 that Michel Mayor and Didier Queloz of the Geneva Observatory announced the discovery of a planet around the solar-type star 51 Pegasi. This discovery represented the first detection of an extrasolar planet around a typical star.[6] Within one month of the announced discovery of 51 Peg, Geoffery W. Marcy and R. Paul Butler of the University of California, Berkeley, and the Carnegie Institution of Washington, respectively, announced that they had detected planets around two other Sun-like stars, 70 Vir and 47 UMa. By May 2006, just over ten years after the original announcements, 189 extrasolar planets had been discovered orbiting 163 stars that are similar to our own Sun.

This modern discovery of extrasolar planets at such a prodigious rate was made possible by dramatic advances in detector technology, the availability of large-aperture telescopes, and diligent, long-term observing campaigns. Given the huge disparity between the luminosity of the parent star and any orbiting planets, direct observation of a planet has proved very difficult; the planet's reflected light is simply overwhelmed by the luminosity of the star.[7] As a result, more indirect methods are usually required to detect extrasolar planets. Three techniques that have all been used successfully are based on ideas discussed in this chapter: radial velocity measurements, astrometric wobbles, and eclipses.[8] The first method, the detection of radial velocity variations in parent stars induced by the gravitational tug of the orbiting planets has been by far the most prolific method at the time this text was written.

[4]More sophisticated binary star modeling codes are available for download on the Internet or may be purchased. Examples include `WD95`, originally written by Wilson and Devinney and later modified by Kallrath, et al., and `Binary Maker` by Bradstreet and Steelman.

[5]In fact, it is thought that Giordano Bruno (1548–1600), a one-time Dominican monk, was executed for his belief in a Copernican universe filled with an infinite number of inhabited worlds around other stars; recall Section 1.2.

[6]In 1992, Alexander Wolszczan, of the Arecibo Radio Observatory in Puerto Rico, and Dale Frail, of the National Radio Astronomy Observatory, detected three Earth- and Moon-sized planets around a pulsar (PSR 1257+12), an extremely compact collapsed star that was produced following a supernova explosion; see Section 16.7. This discovery was made by noting variations in the extremely regular radio emission coming from the collapsed star.

[7]In April 2004, G. Chauvin and colleagues used the VLT/NACO of the European Southern Observatory to obtain an infrared image of a giant extrasolar planet of spectral type between L5 and L9.5 orbiting the brown dwarf 2MASSWJ1207334–393254. HST/NICMOS was also able to observe the brown dwarf's planetary companion.

[8]Another technique has also been employed in the search for extrasolar planets; it is based on the gravitational lensing of light; see Chapter 17.